Photochemistry of Bromofluorobenzenes

O. Anders Borg,[†] Ya-Jun Liu,[†,‡] Petter Persson,[†] Sten Lunell,[†] Daniel Karlsson,[§] Malin Kadi,[§] and Jan Davidsson*[,§]

Department of Quantum Chemistry, Uppsala University, Box 518, S-751 20 Uppsala, Sweden, Department of Theoretical Chemistry, University of Lund, Chemical Center, P.O.B. 124 221 00 Lund, Sweden, and Chemical Physics, Department of Photochemistry and Molecular Sciences, Uppsala University, Box 579, 751 23 Uppsala, Sweden

Received: January 5, 2006; In Final Form: March 14, 2006

The photochemistry of low lying excited states of six different fluorinated bromobenzenes has been investigated by means of femtosecond laser spectroscopy and high level ab initio CASSCF/CASPT2 quantum chemical calculations. The objective of the work was to investigate how and to what extent light substituents, position on the benzene ring and number, would influence the dissociation mechanism of bromobenzene. In general, the actual position of a fluorine atom affects the dissociation rate to a less extent than the number of fluorine atoms. A clear connection between a lowering of a repulsive $\pi\sigma^*$ relative to a bound $\pi\pi^*$ state and the number of fluorine substituents exists, and the previously suggested model of coupling between dissociation rate and relative location of bound and repulsive state still holds for these molecules. A more elaborate examination of the electronic structure of the excited states in bromobenzenes than previously reported is presented.

Introduction

Elucidation of fundamental reaction dynamics of chemical reactions is an important issue in modern physical chemistry; apart from a pure academic point of view, a detailed understanding of the initial dynamics is a condition for the possibility of actively intervening with and ultimately controlling the outcome of a chemical reaction. The halobenzenes, $C_6H_n-X_{6-n}$ (X = F, Cl, Br, I), have proven to be suitable model systems for identification and studies of intramolecular processes and interactions that control the photodissociation dynamics and have therefore received much experimental and theoretical attention lately. Because the dissociation dynamics is largely influenced by the surrounding molecules in the condensed phase, investigations aiming toward a detailed understanding of intramolecular dynamics have to be performed in the gas phase.

Experimentally, the photodissociation dynamics of monohalobenzenes have been studied in the gas phase by photofragment translational spectroscopy (PTS)[1−7] but also in real time by ultrafast pump−probe spectroscopy combined with time-of-flight (TOF).[8−10] The effect of substituents on the dissociation dynamics of multihalobenzenes has also been studied by PTS[11−15] and by femtosecond spectroscopy.[16−18] Quantum chemical calculations of potential energy surfaces have previously been performed for bromo- and chlorobenzene[19−21] and, recently, also for dibromobenzenes and 1,3,5-tribromobenzene.[22] Several spectroscopic studies of halobenzenes have also been performed.[23−29]

The main dissociation channel of halobenzenes, following an excitation in the far-UV, has been suggested to involve predissociation from the lowest excited singlet state, a delocalized ($\pi\pi^*$) state, to a triplet antibonding ($\pi\sigma^*$ or $n\sigma^*$) state localized on the C−X bond. The strength of the coupling between these states as well as the height of the curve crossing point relative to the excitation energy will to a large extent determine the predissociation rate. In general, the predissociation rate is strongly related to the nature of the halogen atom (because the coupling between the states is mediated by spin−orbit coupling) and to a less extent related to the number of halogen atoms and their positions on the benzene ring. Recently we studied *o*-, *m*-, *p*-dibromobenzene and 1,3,5-tribromobenzene by femtosecond spectroscopy[16] where the effect of an additional bromine atom and its position on the predissociation rate could also be ascribed to a change in spin−orbit interaction. In addition, a second, faster, dissociation channel was observed in *o*- and *m*-dibromobenzenes but not in *p*-dibromobenzene and 1,3,5-tribromobenzene. Guided by calculated potential energy curves and group theory analysis we concluded that the origin of the fast dissociation channel was based on crossings between some low-lying initially excited states and some repulsive states and that the difference in the number of experimentally observed channels between different molecules was based on symmetry restrictions for the initial photoexcitation and the low-energy crossings.[22]

The objective of the present work is to investigate the substituent effect in bromobenzenes further. We now focus on the fluorinated bromobenzenes shown in Figure 1, a case where the spin−orbit interaction should be least effected by the fluorine substituent and, thus, where the dissociation rate is controlled by other types of interactions. In the paper we present experimental UV absorption spectra and photodissociation rates, determined by femtosecond pump−probe spectroscopy in molecular beams, for six fluorinated bromobenzenes together with quantum chemical calculations of the relevant potential energy curves (PEC) for these molecules. The theoretical

* Corresponding author. Tel: +46 18 471 36 53. Fax: +46 18 471 36 54. E-mail: jand@fotomol.uu.se.
[†] Department of Quantum Chemistry, Uppsala University.
[‡] Department of Theoretical Chemistry, University of Lund.
[§] Chemical Physics, Department of Photochemistry and Molecular Sciences, Uppsala University.

10.1021/jp0600864 CCC: $33.50
Published on Web 05/11/2006

calculations presented are intended to give a picture of which electronic states are involved in the photodissociation. Highly accurate vertical excitation energies are presented and a simple qualitative relation between absorption wavelengths and dissociation rate is found. The presented crossing points between potential energy curves of orthogonal states correspond to conical intersections as described in refs 30 and 31.

Experimental Details

The experimental arrangement basically consists of an amplified Ti:sapphire femtosecond laser system, a molecular beam apparatus and a time-of-flight mass spectrometric detector (TOF-MS). This setup has been used in previous studies of aryl halides and is described in detail elsewhere; see, e.g., refs 16 and 32. Below follows just a brief overview.

In this setup, the fundamental output from the 1 kHz regenerative amplifier was divided into two fractions with a beam splitter. One fraction generated the 270 nm pump pulses by tripling the fundamental output using two BBO crystals which where 1 and 0.4 mm thick. The other fraction was used to pump an optical parametric amplifier (TOPAS, Light Conversion), which generates the 547 nm probe pulses by sum and frequency mixing of the idler and the fundamental. A variable time delay between the pump and probe pulses was obtained by changing the path length of the probe pulse using a retroreflector mounted on a translational stage. The pulse duration in the present experiments was about 150 fs.

The pump and the probe beams were focused by a spherical plano-convex lens and spatially overlapped with the molecular beam. The plane of polarization of the probe light was oriented perpendicular to the molecular beam whereas the pump polarization could be varied by a Berek compensator. In these experiments, the relative polarization of the pump and probe pulses was kept at the magic angle, i.e., 54.7°.

An effusive molecular beam was produced by heating the oven's chamber to 300−340 K, the variation depending on the vapor pressure of the compound, whereas the exit aperture, with a diameter of 0.2 mm, was kept 20 K higher to prevent condensation. In the pump−probe experiments a boxcar integrator was used to select the desired ionic species. The ion signal was averaged over typically 10 000 laser shots per time delay.

Liquid and gas-phase absorption spectra of all compounds were measured using a conventional spectrophotometer (Perkin-Elmer Lambda 2). Typical concentrations for the liquid-phase measurements were around 4 mM. The gas-phase absorption spectra were measured in a 1 mm quartz cell heated to 333 K.

The chemicals were purchased from commercial retailers, 1-bromo-3,5-difluorobenzene, 1-bromo-2,6-difluorobenzene and bromopentafluorobenzene from Sigma-Aldrich and the other substances from Lancaster Synthesis and used as received.

Computational Methods

All calculations were carried out with the MOLCAS 5.4[33] suite of programs. The complete active space self-consistent field[34] (CASSCF) method was used for geometry optimizations and to obtain reference wave functions to be used in the determination of vertical excitation energies. Accurate calculations of vertical excitation energies require more dynamic electron correlation than CASSCF provides.[35] Therefore the multiconfigurational second-order perturbation theory (CASPT2)[36,37] was employed for this purpose.

The small atomic natural orbital basis set ANO-S[38] included in the MOLCAS 5.4 program package with the contractions (7s3p)/[2s1p], (10s6p3d)/[3s2p1d], and (10s6p3d)/[3s2p1d] was utilized for hydrogen, carbon, and fluorine, respectively. For bromine, the relativistic effective core potential (ECP) basis set with seven electrons (contraction (9s8p4d)/[1s1p2d]) by Barandiaran and co-workers,[39] also included in the MOLCAS 5.4 program package, was used.

One-dimensional potential energy curves (PEC's), describing the variation of the electronic energy as a function of the carbon−bromine distance, were calculated for each of the six molecules under consideration. First, constrained ground-state geometry optimizations of the molecules with the internal C−Br degree of freedom frozen to different values in the range of about 1.3−4.0 Å were carried out. All other degrees of freedom were optimized with respect to the energy within the point group symmetry of the molecule in question.

Next, single point multistate CASPT2 (MSCASPT2) calculations including the three lowest roots in each irreducible representation were performed on the constrained ground-state geometries for both singlet and triplet multiplicity. This procedure should result in vertical excitation energies with errors no larger than 0.3 eV.[35] Accordingly, 24 states were calculated for the molecules belonging to the C_{2v} point group, and 12 states for the C_s dittos. It should be noted that the states calculated this way do not necessarily corresponds to the overall 24 or 12 lowest states. The same level shift was used in all calculations.

Geometrical information of certain low-lying excited states was provided through geometry optimizations constrained to the same symmetry as the ground state.

The 2-bromofluorobenzene and 3-bromofluorobenzene were constrained to C_s symmetry and kept planar in all calculations on the C−Br fragmentations. Labeling the active orbitals (a'_{occ}, a''_{occ}) (a'_{virt}, a''_{virt}) the following active spaces were used: (2, 4) (2, 4) with 12 active electrons for 2-bromofluorobenzene, and (2, 3) (4, 4) with 10 active electrons for 3-bromofluorobenzene.

C_{2v} symmetry was imposed on all calculations on 4-bromofluorobenzene, bromo-2,6-difluorobenzene, bromo-3,5-difluorobenzene, and bromopentafluorobenzene. That is, the calculations were made under the assumption that the two orthogonal mirror planes found in the molecule in its relaxed ground state conformation are retained during the course of the C−Br fragmentation. Labeling the orbitals ($a_{1,\mathrm{occ}}$, $b_{1,\mathrm{occ}}$, $b_{2,\mathrm{occ}}$, $a_{2,\mathrm{occ}}$) ($a_{1,\mathrm{virt}}$, $b_{1,\mathrm{virt}}$, $b_{2,\mathrm{virt}}$, $a_{2,\mathrm{virt}}$) the following active spaces were used: 4-bromofluorobenzene: (1, 2, 1, 1) (2, 2, 2, 2) (10 active electrons), bromo-2,6-difluorobenzene: (1, 3, 1, 1) (2, 2, 1, 1) (12 active electrons), bromo-3,5-difluorobenzene: (1, 2, 1, 2) (1, 2, 1, 1) (12 active electrons), and finally bromopentafluorobenzene: (1, 3, 1, 1) (2, 2, 1, 2) (12 active electrons).

Results

Absorption. Experimental absorption spectra of the bromofluorobenzenes studied are shown in Figures 2 and 3. For comparison, bromobenzene and fluorobenzene have also been included.

Vertical excitation energies, experimental and calculated, of the lowest excited states (the ^1L_b bands using the Platt notation for benzene[40]) of each molecule, are listed in Table 1 together with an estimate of the accuracy of the calculations. The root mean square deviation (RMSD) for the calculation of the first excited state are 0.055 eV compared to experimental results on 0−0 transitions, implying that the accuracy of these calculations are well beneath the 0.3 eV reported in, e.g., ref 35. For the second excited state (the ^1L_a bands) the error is 0.088 eV. The calculated vertical excitation energy of 3-BrFPh seems to be anomalous compared to the experimental energy in 3-BrFPh

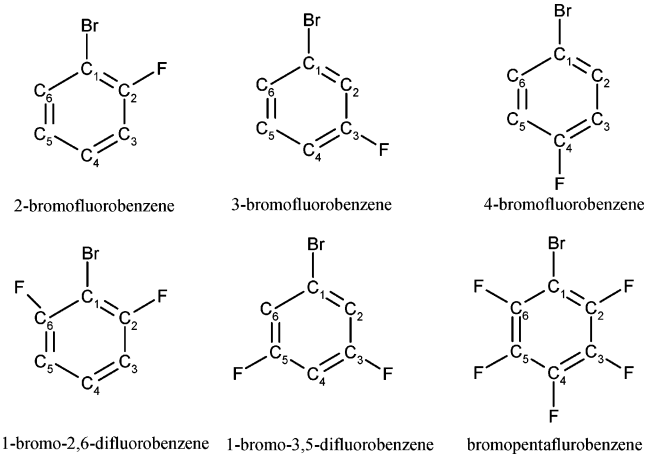

Figure 1. Bromofluorobenzenes investigated in this work.

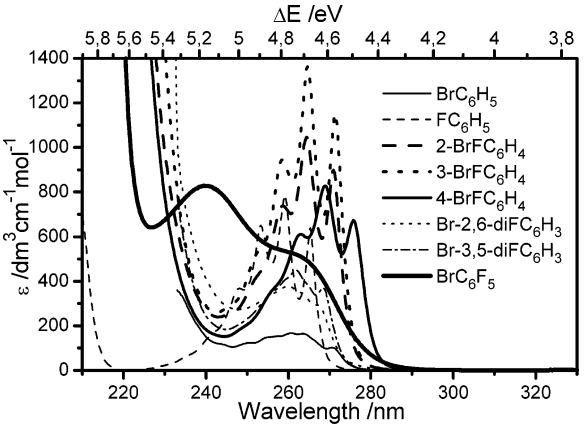

Figure 2. Absorption spectra in acetonitrile showing the ^1L_b-bands. Typical sample concentrations are 4×10^{-3}mol dm^{-3}.

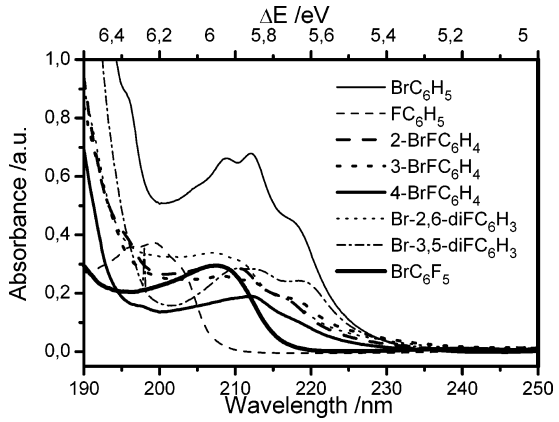

Figure 3. Gas-phase absorption spectra showing the ^1L_a-bands. The intensity of this band is approximately 10 times stronger than the ^1L_b-band.

as well as the calculated energies of 2-BrFPh and 4-BrFPh and has therefore been excluded in this analysis.

All calculated excitation energies as well as major configurations of the respective states can be found in Table 1a−fS. In Table 1, it can be seen that the vertical excitation energies of the lowest exited singlet vary within a small range for all the fluorinated bromobenzenes, i.e., from 4.51 eV for 4-BrFPh to 4.68 eV for BrF_5Ph.

The assignment of the experimental absorption peaks to the calculated vertical excitation energies was based solely upon the energetic order of the CASPT2 roots. Because all lower excitations energies correspond to $n/\pi \rightarrow \pi^*/\sigma^*$ transitions and all orbitals involved in these transitions are included in the active space none of the lowest roots corresponding to 0−0 transitions in the absorbance spectra reported here is missing.

The spectra of all the di- and trisubstituted bromofluorobenzenes show the same main features. They consist of a band between 200 and 230 nm and a less intense band between 245 and 280 nm with vibronic features. The ab initio calculations show that the ^1L_a-band corresponds to excitation of the first singlet $^1\pi\pi^*$ state and the ^1L_b-band corresponds to the second singlet $^1\pi\pi^*$ state. In the case of bromopentafluorobenzene, the S_1 state does not show the same vibronic features and the S_2 state has come down to 240 nm. The peak at 208 nm (both experimentally and calculated) is identified as the third excited singlet ($^1\pi\pi^*$) state.

Looking more closely at the ^1L_a-band, the disubstituted molecules are all similar to fluorobenzene having three significant peaks. For 2- and 3-BrFPh, the 0−0 transition is located at 271.0 and 271.4 nm, respectively. These values are similar to gas-phase measurements giving 270.5 nm for 2-BrFPh[26] and 270.7 nm for 3-BrFPh[27] and in good agreement with the calculated values of 268 and 265 nm. In the case of 4-BrFPh the 0−0 transition is at slightly longer wavelengths, 275.8 or 276.2 nm in the gas phase[28] and with a calculated value of 275 nm. The trisubstituted Br-diFPhs have a ^1L_a-band looking more similar to BrPh, but with a slightly larger absorption coefficient. The 0−0 transitions in 1-Br-3,5-diFPh is at 268.3 nm (267.9 nm in the gas phase[29]) and at 267.1 nm for 1-Br-2,6-diFPh. The agreement with calculated values are even here quite impressive, 264 nm for 1-Br-3,5-diFPh and 267 nm for 1-Br-2,6-diFPh.

Bromopentafluorobenzene lacks the vibronic features in the ^1L_b-band, which can be explained by the calculations which assigns a $^1\pi\sigma^*$ electronic structure to this state.

Orbital Assignment. Relevant, that is with occupation numbers significantly changing during the reactions investigated, CASSCF orbitals of two ground-state optimized molecules from different symmetry point groups, 4-bromofluorobenzene (C_{2v} symmetry) and 3-bromofluorobenzene (C_s symmetry) respectively, are plotted in Figures 4 and 5, respectively, together with CASPT2 energies.

Inspection of basis function coefficients as well as major configurational weights of the wave function (Table 1a−fS where also calculated vertical excitation energies can be found) made classification of the electronic states possible. Calculated low excitation energies together with measured absorption energies of low lying singlets are found in Table 1.

The experimentally observed dissociation dynamics of fluorinated bromobenzenes through excitation to low lying excited states can be attributed to a transition between the lowest lying $\pi\pi^*$ states of the benzene ring and a dissociative $\pi\sigma^*$ or $n\sigma^*$ state, where σ^* is the antibonding C−Br orbital. In this work, the lowest repulsive state is best described as $\pi\sigma^*$ and not $n\sigma^*$, as opposed to what has been reported for iodobenzenes.[8] The bromine in-plane lone pair lies lower in energy than the overall HOMO. At the optimized ground state geometry the bromine out-of-plane electron pair is in principle not mixed with the HOMO, which is essentially a π-orbital. In 4-bromofluorobenzene for example, H (L) referring to HOMO (LUMO) within that particular irreducible representation, this bromine p-orbital is essentially the b_1 (HOMO−2) molecular orbital whereas b_1 (HOMO), which is the overall HOMO, in essence is a pure benzene π−orbital. This ordering is changed during the course of the reaction and as the molecule fragments the bromine lone pair ends up as b_1 (HOMO). Note that n in this paper in $n\sigma^*$

TABLE 1: Measured Absorbance Maxima and Calculated Vertical Excitation Energies

	2-BrFPh				3-BrFPh				4-BrFPh				1-Br-2,6-FPh				1-Br-3,5-FPh				BrF_5Ph				
	CASPT2		exp		CASPT2		exp		CASPT2		exp		CASPT2		exp		CASPT2		exp		CASPT2		exp		RMSD[a]
state	eV	nm	eV	nm	eV	nm	eV	nm	eV	nm	eV	nm	eV	nm	eV	nm	eV	nm	eV	nm	eV	nm	eV	nm	eV
$^3\pi\pi^*$	3.84	323			3.88	320			3.83	324			3.86	321			3.94	314			3.85	322			
$^3\pi\pi^*$	4.40	282			4.45	279			4.11	302			4.45	279			4.48	277			4.51	275			
$^3\pi\pi^*$	4.46	278			4.51	275			4.44	279			4.49	276			4.57	271			4.52	274			
$^1\pi\pi^*$	4.62	268	4.60	271	4.67	265	4.57	271	4.51	275	4.50	276	4.65	267	4.64	267	4.69	264	4.62	268	4.68	265	4.70	264	0.055
$^3\pi\sigma^*$	5.51	225			5.48	226			5.58	222			5.37	231			5.44	228			4.91	253			
$^1\pi\sigma^*$	5.85	212	5.74	216	6.49	191	5.71	217	5.96	208			5.83	213			5.78	215	5.66	219	5.23	237	5.17	240	0.327[b]
$^1\pi\pi^*$	6.30	198			6.75	184			5.80	214	5.74	216	5.80	214	5.74	216	5.84	212			5.97	208			0.088[c]

[a] Root mean square deviation. [b] RMSD including 3-fluoro. [c] RMSD excluding 3-fluoro.

$$\mathrm{RMSD} = \sqrt{\frac{\sum_{\text{molecules}} (T_v^{\text{exp}} - T_v^{\text{CASPT2}})^2}{N}}$$

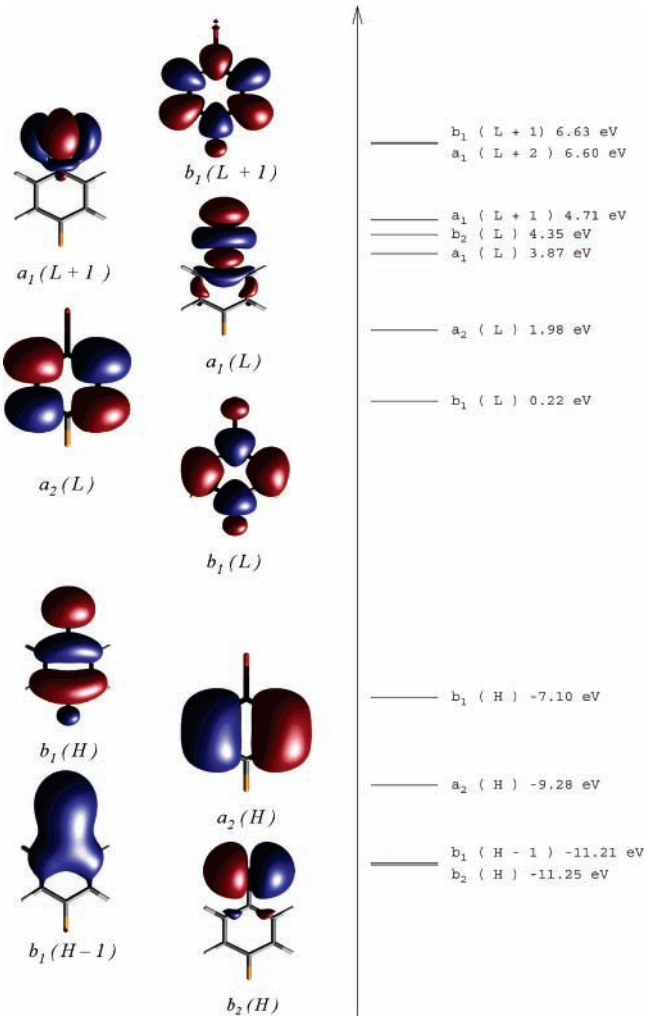

Figure 4. CASSCF orbitals of 4-bromofluorobenzene relevant for the chemistry under consideration in this paper together with CASPT2 energies.

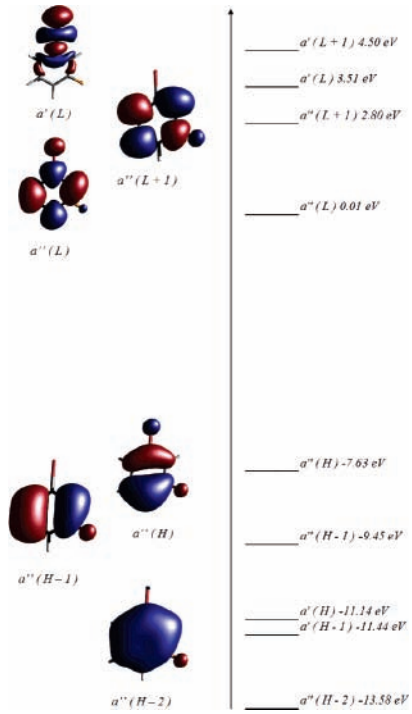

Figure 5. CASSCF orbitals of 3-bromofluorobenzene relevant for the chemistry under consideration in this paper together with CASPT2 energies.

refers to the in-plane lone pair in bromine, which does not mix with the π-orbitals of the phenyl ring. The model with a transition from a bound $\pi\pi^*$ state to a repulsive one is consistent with computational studies reported for related aryl halides by Liu et al.[22,30]

It has been suggested by Griffiths et al.[41] and Kavita et al.[42] that a charge transfer (CT) state originating from an $n \rightarrow \pi^*$ transition might be of relevance for the photodissociation of fluoroiodobenzenes. This is of no importance for the processes and molecules investigated here because these CT states are energetically well outside the range of the photochemistry considered in this work. From Table 1(a−f)S it can be deduced that the overall lowest lying bound charge transfer state is found in 4-BrFBz at 6.93 eV, well above the first bound singlet state at 4.51 eV.

Orbitals in C_{2v} Symmetry. The computations show that HOMO and LUMO embrace b_1 symmetry and that HOMO−1 and LUMO+1 belongs to the a_2 irreducible representation. This is of interest because the energetic ordering of the orbitals is closely related to the calculated configurations representing the three lowest excited triplet states, which are all of ($\pi \rightarrow \pi^*$) type. The major configurations building up these triplets are, from lower to higher energy, $b_1(H) \rightarrow b_1(L)$ (A_1 symmetry for the total state), $b_1(H) \rightarrow a_2(L)/a_2(H) \rightarrow b_1(L)$ (B_2 symmetry) and $a_2(H) \rightarrow a_2(L)$ (A_1 symmetry), implying a qualitative connection between the relative order of the orbital energies and excitation energies with low orbital energy differences yielding low excitation energies and vice versa. The corresponding singlet states are, due to exchange interaction, higher

TABLE 2: Crossing between First Excited Bound Singlet and Relevant Repulsive States for Molecules Belonging to C_{2v} Symmetry Point Group[a]

	dist (Å)/energy rel S_1-B_2 (eV)/energy rel S_0 (eV)					
	2-BrFPh	3-BrFPh	4-BrFPh	1-Br-2,6-FPh	1-Br-3,5-FPh	BrF_5Ph
$^3\pi\sigma^*$	2.08/0.24/4.83	2.09/0.21/4.80	2.10/0.14/4.73	2.03/0.18/4.77	2.07/0.30/4.89	1.97/0.14/4.73
$^1\pi\sigma^*$	2.13/0.31/4.90	2.14/0.32/4.91	2.15/0.25/4.84	2.09/0.31/4.90	2.11/0.41/5.00	2.02/0.20/4.79
$^3n\sigma^*$			2.18/0.31/4.90	2.11/0.36/4.95	2.13/0.45/5.04	2.08/0.31/4.90
$^1n\sigma^*$			2.23/0.48/5.07	2.16/0.49/5.08	2.18/0.59/5.18	2.14/0.47/5.06

[a] For the C_s dittos the estimated crossing points are presented

in energy than the triplets.[43] The first B_2 ($b_1(H) \rightarrow a_2(L)/a_2(H) \rightarrow b_1(L)$) singlet is, accordingly, a little higher in energy than the corresponding triplet and is also the fourth excited state of these molecules. The singlet−triplet splitting is much more pronounced for the two A_1 states than for the B_2 ditto.

The repulsive T_1-B_1 and S_1-B_1 states are represented by $b_1(H) \rightarrow a_1(L)$ and $b_1(H-1) \rightarrow a_1(L)$ configurations, that is a $\pi\sigma^*$ electronic configuration. The repulsiveness of this state is in concordance (Table 1) with the presence of a nodal plane between carbon and bromine in $a_1(L)$, as indicated in Figure 4. The C−Br distance as well as the energy of the crossing point between these two states and the bound geometrically optimized first excited singlet state in the one-dimensional potential energy curves presented here are included in Table 2. The repulsive singlet and triplet variants of the $n\sigma^*$ electronic states (with largest configurational weight for the $b_2(H) \rightarrow a_1(L)$ excitation) might also be of interest for the low energetic dissociation mechanism of these molecules.

C_s Molecules. As for the C_{2v} molecules, three triplet states are found with lower energy than the lowest lying singlet and all four are ($\pi \rightarrow \pi^*$) excitations. For these molecules, however, the first and third triplet are represented by $a''(H-1) \rightarrow a''(L)$ and $a''(H) \rightarrow a''(L+1)$ configurations and the second by $a''(H) \rightarrow a''(L)$ and $a''(H-1) \rightarrow a''(L+1)$. According to Figure 5, $a'(L)$ has a nodal plane between the carbon and the bromine, something that is also true for $a'(L+1)$. This indicates that the T_1-A'' and S_1-A'', which are represented by $a''(H)/a''(H-1)$-$(\pi) \rightarrow a'(L)/a'(L+1)(\sigma^*)$ configurations, should be repulsive, something that is also seen in the PEC's presented later in this work. Further, only 2-BrFPh and 3-BrFPh lack a C_{2v} axis and a comparison between 3-BrFPh and 4-BrFPh shows that the molecular orbitals retain approximately the same shapes as with the C_{2v} symmetry and that the bromine has a larger influence on the nodal structure than the fluorine, which appears to present a weaker perturbation to the benzene molecular orbitals. It is also clear that the C−Br (σ^*) bond lies lower in energy than C−F (σ^*), and this is important when determining which bond is easiest to dissociate.

Photodissociation. The dissociation rate of the aryl halides in the molecular beam were followed by monitoring the formation of ions produced by the pump and probe pulses. One pump photon (270 nm, 4.59 eV) excites the molecules and two, or more, subsequent probe photons (547 nm, 2.27 eV) bring the excited molecules above the ionization limit.

Multiphoton excitation of the ground-state contributes to a constant ion background signal. However, low intensities were used in the time-resolved experiments to ensure that the main ionization pathway is the pump−probe process.

Figure 6 shows the time-of-flight mass spectra of the molecules recorded with the pump pulse. In these spectra, the intensity was much higher than in the time-resolved experiments.

Results from the time-resolved measurements showing the intensity of the molecular ion signal as a function of the delay between pump and probe pulses are displayed in Figure 7.

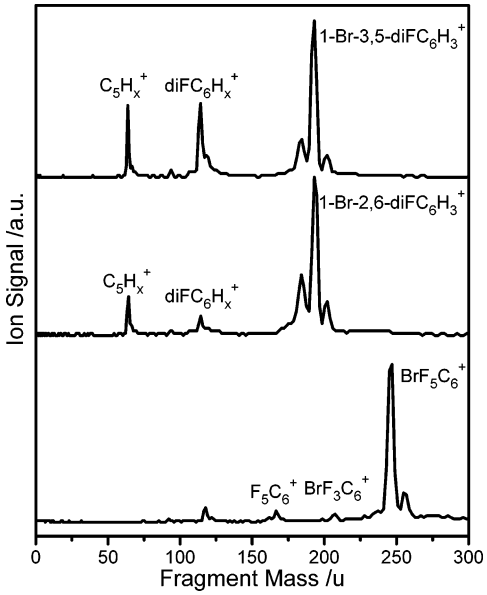

Figure 6. Time-of-flight spectra recorded with the pump.

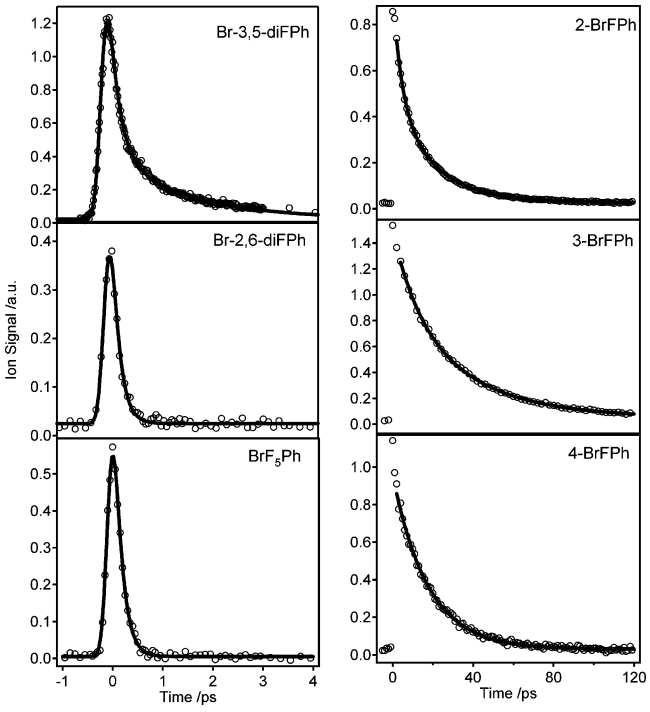

Figure 7. Ion signal versus delay time. The pump signal has been subtracted from pump−probe signal.

In addition to the pump−probe ion signal, the ion signal from the pump itself was recorded. Prior to data analysis, this pump ion signal was subtracted from the pump−probe ion signal to correct for fluctuations of the laser intensity and variations in the density of molecules in the molecular beam.

The kinetic traces of 2-, 3- and 4-BrFPh were fitted with an exponential decay function. The fast decay traces of BrF_5Ph, 1-Br-2,6-diFPh and 1-Br-3,5-diFPh, were fitted with a Gaussian for the response function, fwhm 225 fs, and an exponential decay function. To achieve a good fit for 1-Br-3,5-diFPh, 2-BrFPh and 3-BrFPh, it was necessary to employ two time constants, τ_1 and τ_2, in the analysis. The decay curves are shown in Figure 7, and the average of the best fit parameters are summarized in Table 3 together with previously published data for the bromobenzene.[9,16]

High level ab initio calculations with the aim of elucidating the photodissociation mechanism of halogenated benzenes have previously been reported in, for example, refs 20−22. Here we are using the same approach but focusing on a deeper understanding of the electronic states involved in the dissociation process and on the effect of the secondary, in this case fluorine, substituent.

Important bond lengths of low lying excited states are listed in Table 2S; the numbering of the atoms refers to the numbering in Figure 1. It can be noted that all changes in bond lengths upon excitations are small, the largest being +0.106 Å (C_2-C_3 in T_1-A_1 in 4-BrFPh). In essence, the change in bond lengths upon excitation can be traced down to the nodal structure of the respective orbitals involved; see Figures 4 and 5. The most striking example can be found in the C_2-C_3 bond in the first triplet state (T_1); this bond is elongated in 4-BrFPh (+0.106 Å) where the major configuration is $a_2(H) \rightarrow a_2(L)$ ($w = 0.47$) with introduction of a node in the C_2-C_3 bond, to be compared with the corresponding change in bond length in 1-Br-2,6-FPh (−0.039 Å), 1-Br-3,5-FPh (−0.040 Å) and BrF_5Ph (−0.042 Å) where the dominant configuration is $b_1(H) \rightarrow b_1(L)$ ($w = 0.51$, 0.47, and 0.50; see Table 1d−fS) with introduction of a node in the C_1-C_2 bond. This leads to elongation of that bond (+0.073 Å in 1-Br-2,6-diFPh and 1-Br-3,5-diFPh and +0.079 Å in BrF_5Ph). The first excited singlet state is represented by $H - 1 \rightarrow L/H \rightarrow L + 1$ in all molecules with increased number of nodes. Accordingly, the bond lengths are slightly elongated, with alterations in the range from +0.034 Å for C_5-C_6 in 3-Br−FPh and C_1-C_2 in 2-Br−FPh to +0.059 Å for C_1-C_2 in BrF_5-Ph.

The approach chosen in the above-mentioned works by Liu et al. to asses the dissociation kinetics was to calculate one-dimensional PEC's varying the C−X distance, X representing the leaving halogen atom. One of the claims in these previous papers is that the value of the dissociation constant is often connected to the location of the crossing point in the PEC's between the first bound $\pi\pi^*$ singlet and the first repulsive triplet and the coupling between them. The coupling between the singlet and triplet states should essentially be governed by spin−orbit interaction. In the molecules included in this investigation it can be assumed[43] that the dominant contribution to spin−orbit interaction is due to the presence of the bromine. Therefore the coupling strength was assumed to be about the same in all molecules. Following the approach and discussion by Liu et al.,[20−22] the remaining parameter is the location of the crossing point between the potential energy surfaces. In this work the one-dimensional potential curves were calculated, primary to find out which electronic states that are involved in the dissociation but also to see if the connection between the number of substituents and a lowering of the repulsive states reported above is reflected in the location of the crossing points.

Adiabatic potential energy curves from the calculations, as well as selected diabatic ones, can be found in Figure 8. Only the curves necessary to study the photochemistry of the low lying excited states are included.

As already stressed, the lowest lying excited states in these fluorinated bromobenzenes correspond to excitations essentially located in the benzene ring and they therefore only cause minor alterations of the C−Br bond. This can be seen in the one-dimensional potential energy surfaces presented here because the four lowest lying excited potential energy curves for the C−Br degree of freedom are essentially isomorphic with the corresponding S_0 curve. Four repulsive curves are included in the diabatic PEC's of the molecules belonging to the C_{2v} irreducible representation. These repulsive states cross the bound S_1-B_2 state at moderately low energies and are therefore potentially interesting when unraveling the dissociation dynamics attributed to the interaction between the low lying excited states.

From the PEC's we can conclude that the dissociation mechanism in all these molecules correspond to $\pi\pi^* \rightarrow \pi\sigma^*$ and not $\pi\pi^* \rightarrow n\sigma^*$ transitions and that this is by no means affected by the number of fluorines or their location relative to bromine.

Bromofluorobenzenes. The dissociation channel present in all disubstituted bromofluorobenzenes is represented by the τ_1 time constant and corresponds to a transition between the bound S_1 state and a repulsive T state, i.e., the same channel as the one observed earlier for many halobenzenes. Crossing points related to the optimized first excited singlet between the bound $\pi\pi^*$ and the repulsive states are listed in Table 2. The energy of the crossing points between S_1-B_1 and T_1 ($^3\pi\sigma^*$) are 0.24, 0.21, and 0.14 eV for 2-, 3-, and 4-BrFPh, respectively. The variation of the crossing point energies between these molecules is small and not correlated to the variations in dissociation rate. Thus some other mechanism, not represented in the present PECs, must dominate the coupling between the states.

The presence of a second time constant, τ_2, as in 2- and 3-BrFPh, indicates that an additional electronic state is initially excited. In addition, this is in accordance with the dibromobenzenes, were a second channel was also observed for 2,3-dibromobenzene but not for 4-dibromobenzene.[16,22] In the dibromobenzenes, τ_2 was assigned to a channel involving an excitation to a predissociative triplet state with a sufficiently low barrier to allow for dissociation. The corresponding barrier for 4-diBrPh was too high to allow direct dissociation.

The potential energy curves for the bromofluorobenzenes in Figure 8 shows that with the employed excitation energy only one singlet state is accessible and therefore the second state initially excited must be a triplet. Excitation to triplet states is allowed when there is a singlet state with proper symmetry lying energetically close.[43] Accordingly, in 2- and 3-BrFPh, T_2-A' or T_3-A' is most likely excited. The T_2-A' state has a barrier for dissociation at roughly the same energy as the S_1-A' to T_1-A'' ISC point. Therefore we suggest that the fast channel corresponds to dissociation via the T_2-A' state. In the 4-BrFPh, however, excitation of the T_1-B_2 state, which corresponds to the dissociative T_2-A' state in 2- and 3-BrFPh, is forbidden according to symmetry restrictions. The only adjacent triplet state in 4-BrFPh is the bound T_2-A_1 state, which could explain the absence of a fast channel in this molecule.

Di- and Pentafluorobromobenzenes. The dissociation constants for 1-Br-3,5-diFPh, 1-Br-2,6-diFPh and BrF_5Ph are at least 10 times faster than those for the disubstituted bromofluorobenzenes. The calculated S−T crossing points are 0.30, 0.18 and 0.14 eV and the dissociation constants 1.9, <0.3, <0.3 ps for 1-Br-3,5-diFPh, 1-Br-2,6-diFPh and BrF_5Ph, respectively. Thus,

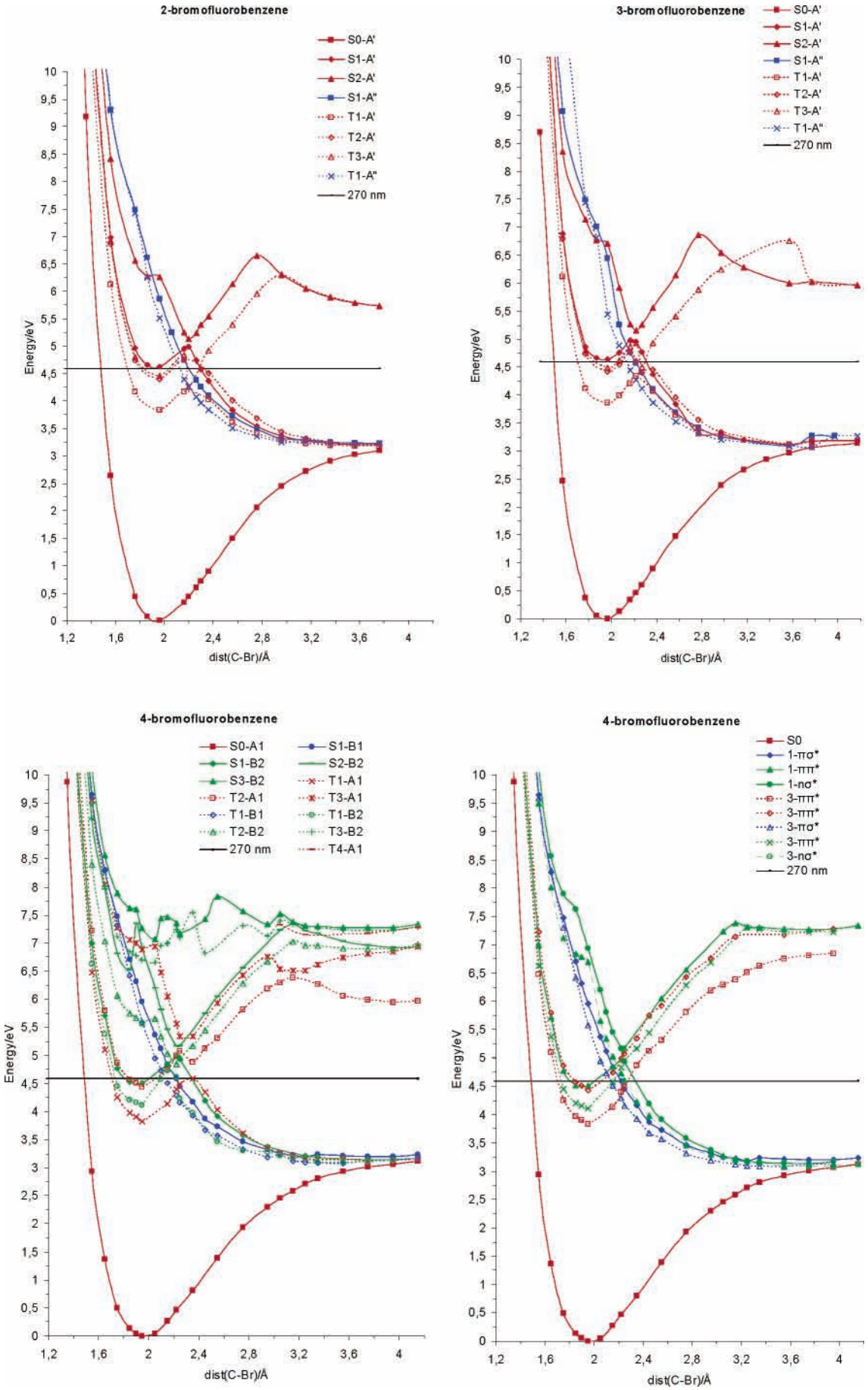

Figure 8 cont'd.

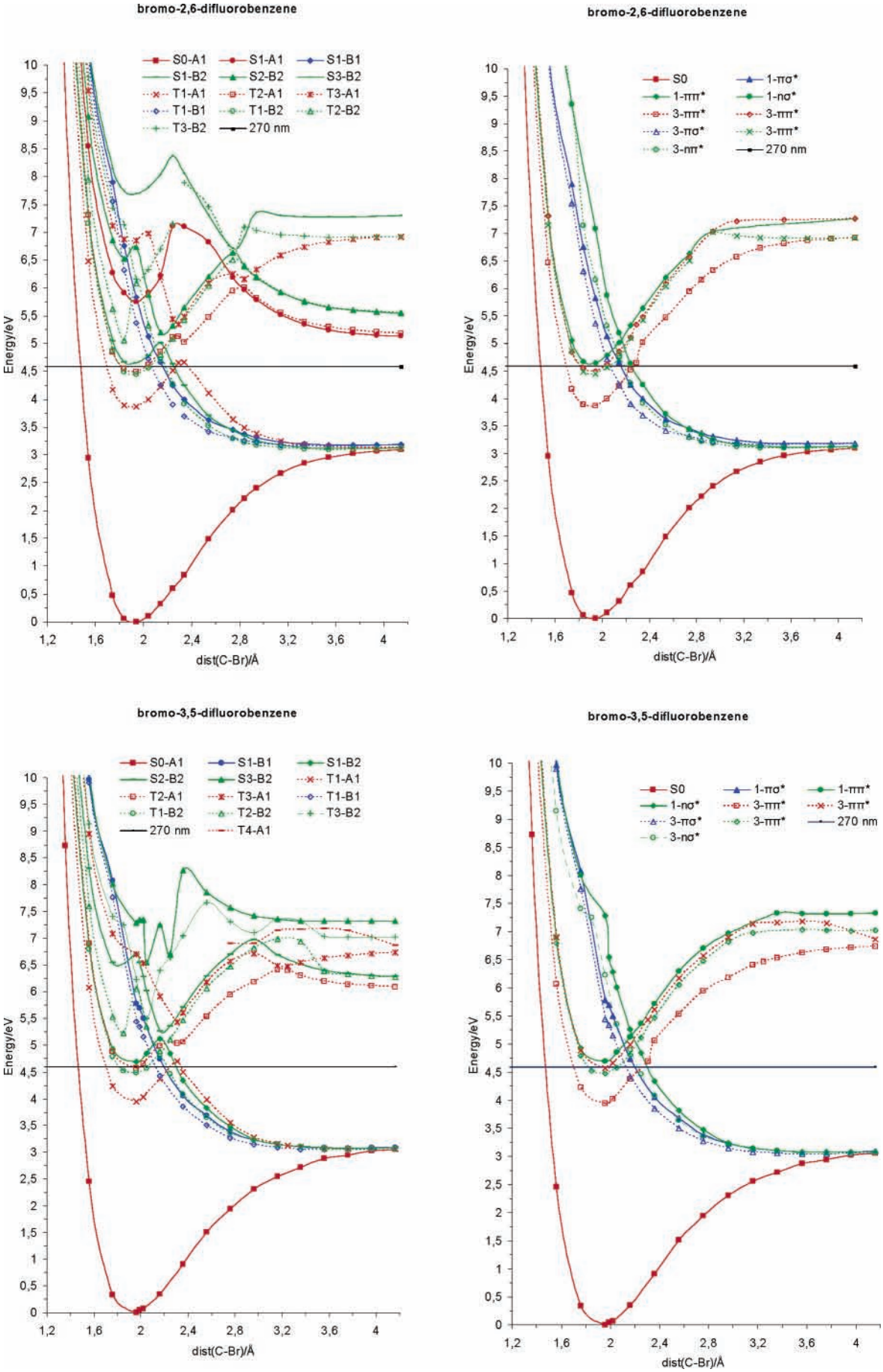

Figure 8 cont'd.

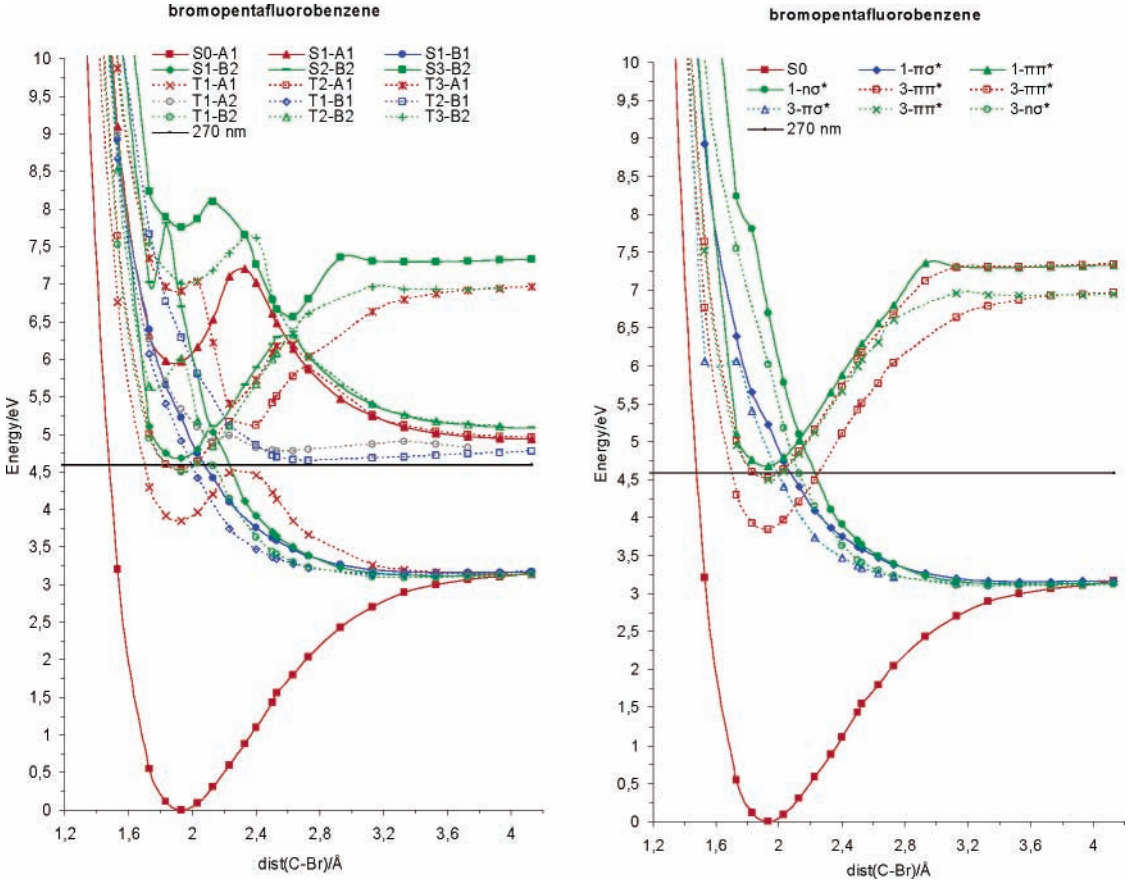

Figure 8. Adiabatic potential energy curves of the lowest states of all molecules included in this work as well as diabatic dittos for the molecules embracing C_{2v} symmetry.

TABLE 3: Dissociation Time Constants and Relative Amplitudes for the Aryl Halides Excited with 270 nm

	A_1	τ_1/ps	A_2	τ_2/ps
BrC_6H_5[a]	1	26 ± 2		
2-$BrFC_6H_4$	0.5	20.8 ± 3.1	0.5	5.6 ± 2.9
3-$BrFC_6H_4$	0.5	44.1 ± 4.0	0.5	15.6 ± 5.1
4-$BrFC_6H_4$	1	19.5 ± 2.3		
1-Br-3,5-diFC_6H_3	0.8	1.9 ± 0.3	0.2	<1
1-Br-2,6-diFC_6H_2	1	<0.3		
1-BrC_6F_5	1	<0.3		

[a] Results taken from Kadi et al.,[9] measured at 266 nm.

in contrast to the disubstituted molecules,[16,22] the dissociation rates are seemingly reflected by the energetic lowering of the repulsive state and the crossing points. However, the dissociation of 1-Br-2,6-diFPh and BrF_5Ph are too fast to be assigned to a predissociation mechanism mediated by spin−orbit coupling. In comparison, iodobenzene exhibit two time constants, 0.7 and 0.35 ps, corresponding to the S−T predissociation channel and a direct excitation of a repulsive state, respectively.[8,9] The fast predissociation of 0.7 ps, about 40 times faster than in bromobenzene, is in iodobenzene motivated by the presence of a heavy iodine atom which creates a strong coupling between the excited singlet and the repulsive triplet state. The dissociations of 1-Br-2,6-diFPh and BrC_6F_5 occur even faster than in iodobenzene and because the bromine is much lighter than iodine it is very unlikely that the dissociations in these molecules occur via the S−T predissociation mechanism. It is rather more likely that a repulsive singlet state is excited directly.

There is a repulsive singlet state in bromopentafluorobenzene, S_1-B_1, which is within reach with the 270 nm pump, according to Figure 8. Excitation directly to a repulsive state is also somewhat supported by the lack of a vibronic structure in the absorption band of bromopentafluorobenzene; see Figure 2. In comparison, the absorption bands in the fluorobenzenes, F_xPh, lose their vibronic structure when going from $x = 1-4$ to $x = 5-6$.[23] This has been assigned to a lowering of the repulsive C−F $^1\pi\sigma^*$, which opens up a direct dissociation channel along the C−F bond.[44] In the TOF mass spectra we see a small peak corresponding to $C_6F_3Br^+$, which actually indicates that the C−F channel is open in bromopentafluorobenzene. In our ab initio calculations we have also seen a tendency of mixing between the $^1\pi\sigma^*$ in the C−F and the S_1-B_1 state along the C−Br in all the difluoro- and trifluoro-substituted benzenes. However, we assign the main dissociation channel in bromopentafluorobenzene to be a direct excitation to the repulsive S_1-B_1 state followed by dissociation along the C−Br bond.

In the case of 1-Br-2,6-diFPh the repulsive singlet state lies higher in energy and it is not that obvious that a laser pulse with 4.59 eV could bring the molecule to this state. However, the experimental fast dissociation rate strongly indicates that the excitation actually takes place directly to a repulsive singlet state, which in turn may suggest that the one-dimensional potential energy curve representation is not sufficient in this case and that a multidimensional potential energy surface, introducing other vibrational modes that may be important, has to be employed before a more detailed analysis can be carried out. Currently, we are working on including this in the analysis.

The repulsive S_1-B_1 state in 1-Br-3,5-diFPh lies even higher in energy, which probably rules out significant population of this state, even if other vibrational modes are included. In addition, this molecule has a clearly discernible vibronic feature in the absorption band even though it is not as pronounced as in the bromoflourobenzenes. Still 1-Br-3,5-diFPh has a relatively

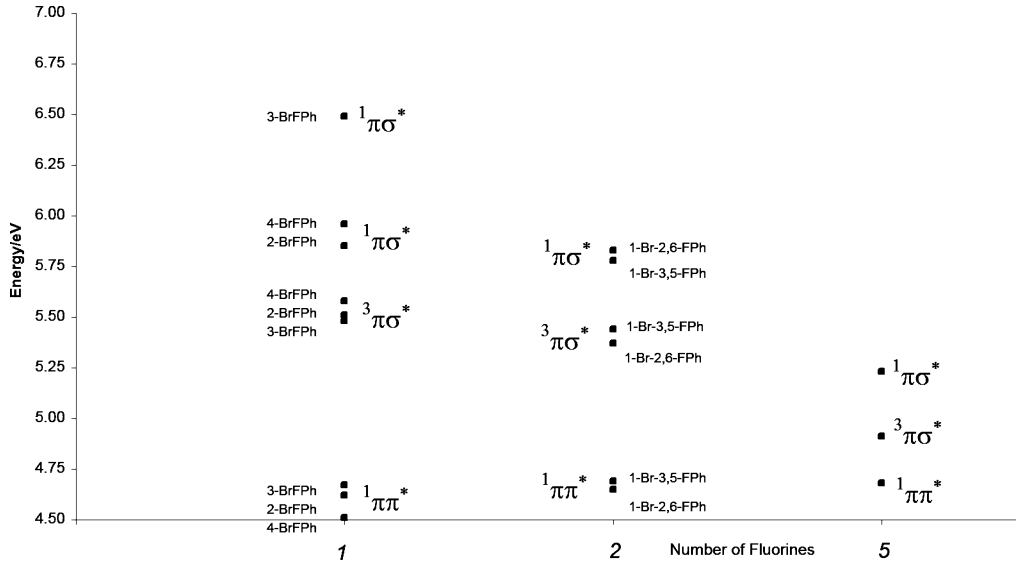

Figure 9. Vertical excitation energies of the lowest lying bound and repulsive states.

short excited-state lifetime, 1.9 ps, compared to the bromofluorobenzenes. In addition, there seems to be a second, subpicosecond, time constant present. The 1.9 ps decay constant is similar in magnitude to the decay constant for 1,3,5-triBrPh,[16] where a substantial lowering of the S−T crossing point connected to a lowering of the dissociation barrier was observed. This, in combination with an increasing spin−orbit coupling, due to the presence of three bromine atoms, motivated the short lifetime in 1,3,5-triBrPh. As already mentioned, the PEC for 1-Br-3,5-diFPh shows no major lowering of the S−T crossing point, which basically rules out a similar mechanism as in 1,3,5-triBrPh. In this case of 1-Br-3,5-diFPh we believe that the small fast component is due to a direct excitation to the repulsive S_1-B_1 and that the 1.9 ps component is due to an excitation to the bound S_1 state where part of the molecules dissociate via the repulsive S_1-B_1 state in competition with the S−T channel. The transition from the bound S_1 to the repulsive S_1-B_1 is symmetry forbidden in C_{2v} but may be facilitated by molecular vibrations.

Discussion

Having considered the absorption spectra and associated photodissociation behavior of a number of fluorinated bromobenzenes individually in depth, it is interesting to look for general trends both among this series, and with respect to related aryl halides. In the following, we discuss the relative importance of different substitutional strategies on photodissociation rates in aryl halides.

It has in previous reports been established that the choice of leaving group is essential for the location of the dissociative potential energy surface with respect to the bound ditto, and that this effect is large enough to be visible in one-dimensional potential energy surfaces describing the total electronic energy as a function of the C−X distance.[20] The largest experimental differences in dissociation rates have also been found between halogenated benzenes containing different leaving groups[9]

For monosubstituted benzenes a factor of as much as 40 in dissociation rate is obtained when moving one step further down in the periodic system. A key step toward a structured description of the dissociation kinetics of halogenated benzenes can accordingly be made by designating the nature of the leaving atom as the primary component in this puzzle.

A second parameter that is explicitly addressed in this work is the influence of the number of substituents on the photochemistry. Calculated vertical excitation energies to the bound $^1\pi\pi^*$ and the repulsive $^3\pi\sigma^*$ and $^1\pi\sigma^*$ states taken from Table 1 are shown for the six investigated bromofluorobenzenes in Figure 9. The figure shows that the difference in energy between on one hand the bound state, and on the other hand the repulsive states decreases with the number of substituents. This effect is evident in, e.g., the absorption spectrum of pentafluorobromobenzene (Figure 2), where the repulsive singlet state is lowered sufficiently to be clearly identifiable experimentally as a distinct absorption feature at 240 nm. At the same time, the experimental photodissociation data in Table 3 shows that the dissociation rates increase with the number of substituents. For example, the dissociation rate is at least a factor of 7 faster for the difluorobromobenzenes than for the monofluorobromobenzenes. A similar trend has been presented also for the pure bromobenzenes,[14] with an increase in dissociation rate with a factor of 2−6 following an increase in the number of substituents. We therefore conclude that the number of substituents is important both for the absorption and for the subsequent dissociation dynamics. Together, the results presented for the excitation and the photodissociation suggest that the observed increase in dissociation rate when more fluorines are added can be ascribed to the systematic lowering of the repulsive states relative to the bound excited states. This effect of fluorine substitution was recently reported for pure fluorobenzenes in ref 20. Here we show that the effect extends also to cases where the primary bond breaking involves another substituent on the benzene.

Given the clear correlation between the calculated vertical excitation energies and the experimental photodissociation rates, the lack of a clearly discernible pattern for the crossing points is somewhat disappointing in the sense that it makes it more difficult to make ab initio predictions about experimental photodissociation rates. As pointed out by Sobolwski and Domcke,[2] it is furthermore likely that a quantitative description of the photodissociation rates will require the location of transition states that depends on several degrees of freedom around the crossing point, which is a conical intersection. It remains to be determined whether the experimental photodissociation variation with the number of substituents on the ring is primarily related to variations in crossing point energies at the true photodissociation transition states or to non-PES effects such as spin−orbit coupling. Work to calculate more accurate

photodissociation transition barriers is in progress and will be reported in due course.

Clearly, the previously reported[20−22] effects where the crossing of potential energy curves is lowered by the primary substituent has the largest influence on the dissociation and should be regarded as the primary factor for the photodissociation dynamics. The effects reported here, even though they are large, should be regarded as secondary.

An even smaller effect for the dissociation rate is the nature of the secondary halogen, that is, which substituents apart from the leaving group are present in the molecule. Again, this effect is not evident in the calculated crossing points between the potential energy curves, although it appears to influence the experimental dissociation constant. A comparison between the dissociation dynamics of fluorobromobenzene and di- and tribromobenzene[22] shows that the dissociation of dibromobenzenes are 3 times faster than the dissociation of 2- and 3-fluoro-substituted bromobenzenes, but that no difference is obtained for 4-substituted molecules. There is also no real difference in dissociation constants for the 1,3,5 substituted benzenes. It can be concluded that this effect is significant for some halogenated benzenes but it depends on the location of secondary substituents with respect to the leaving group.

In this context it should be noted that spin−orbit interaction is most likely more important in molecules containing several bromines than in fluorine-substituted ones,[43] so it is therefore not surprising that the difference in dissociation rate is not captured by the calculations reported here and in ref 21.

It is also interesting to consider the effect of the location of the secondary substituents with respect to the leaving group on the dissociation rate. This parameter is responsible for a factor of maximum about 2 in the experimental dissociation rates for the disubstituted molecules. The effect seems to be larger for the trisubstituted, but the series of molecules investigated is still too small to allow us to draw any conclusions so far. This is a comparatively small effect that is not captured either by the potential energy surfaces reported here or by the calculated vertical excitation energies. Nevertheless, it is can be a significant factor in the experimentally measurable dissociation kinetics of these molecules.

Conclusions

The general conclusion drawn from this work is that in the bromofluorobenzenes the main dissociation channel, following excitation at around 270 nm, is a predissociation involving the bond S_1 state ($\pi\pi^*$) and a repulsive triplet ($\pi\sigma^*$) state, which gives rise to the observed dissociation rates of 20−40 ps. Thus, these molecules have the same main dissociation pathway as all bromobenzenes, except those with a subpicosecond dissociation rate. In di- and pentafluorobenzenes a repulsive ($\pi\sigma^*$) singlet state, S_1-B_1, lies lower in energy, which affects the dissociation mechanism significantly. The very fast dissociation rate in 1-Br-2,6-diFPh and BrF_5Ph (<300 fs) is caused by a direct excitation to this state. In 1-Br-3,5-diFPh the situation is more complicated and we propose a mechanism where both the bound S_1 state and the repulsive S_1-B_1 are excited. In the disubstituted bromofluorobenzenes we also observe a second, faster, dissociation channel in 2- and 3-BrFPh that is missing in 4- BrFPh. Guided by the calculated PEC's we propose that the origin of the fast channel in 2- and 3-BrFPh is based on a dissociation of some low-lying initially excited triplet state over a small barrier. Due to the higher symmetry in 4-bromofluorobenzene this exit channel is forbidden.

This work illustrates that effects due to exchange of the leaving group can be captured by means of calculation of difference in vertical excitation energies between the excited bound and repulsive state. On the basis of the experimental UV absorption spectra, we conclude that the accuracy of the calculations is very good and that the error in the calculated vertical excitation energies is of the order of 0.1 eV. This work also illustrates the limitation of the one-dimensional PEC representation in some cases. Especially in 1-Br-3,5-diFPh and 1-Br-2,6-diFPh we believe that the observed dynamics are related to various internal vibrations in the molecules that can only be explicitly captured in a multidimensional PES representation.

Acknowledgment. The Göran Gustafsson Foundation, the Magnus Bergvall Foundation and Swedish Research Council (VR) are gratefully acknowledged for financial support. The Swedish supercomputer centers NSC and Swegrid are acknowledged for generous supply of computer resources.

Supporting Information Available: Table 1a−fS, vertical excitation energies and the corresponding major configurations of those states. Table 2S, geometrical parameters of some excited states. This material is available free of charge via the Internet at http://pubs.acs.org.

References and Notes

(1) Dzvonik, M.; Yang, S. C.; Bersohn, R. *J. Chem. Phys.* **1974**, *61*, 4408.
(2) Freedman, A.; Yang, S. C.; Kawasaki, M.; Bersohn, R. *J. Chem. Phys.* **1980**, *72*, 1028.
(3) Freitas, J. E.; Hwang, H. J.; El-Sayed, M. A. *J. Phys. Chem.* **1993**, *97*, 12481.
(4) Hwang, H. J.; El-Sayed, M. A. *J. Chem. Phys.* **1992**, *96*, 856.
(5) Zhang, H.; Zhu, R.-S.; Wang, G.-J.; Han, K.-L.; He, G.-Z.; Lou, N.-Q. *J. Chem. Phys.* **1999**, *110*, 2922.
(6) Ichimura, T.; Mori, Y.; Shinohara, H.; Nishi, N. *Chem. Phys. Lett.* **1994**, *189*, 117.
(7) Ichimura, T.; Mori, Y.; Shinohara, H.; Nishi, N. *Chem. Phys. Lett.* **1985**, *122*, 51.
(8) Cheng, P. Y.; Zhong, D.; Zewail, A. H. *Chem. Phys. Lett.* **1995**, *237*, 399.
(9) Kadi, M.; Davidsson, J.; Tarnovsky, A. N.; Rasmusson, M.; Akesson, E. *Chem. Phys. Lett.* **2001**, *350*, 93.
(10) Wilkerson, C. W., Jr.; Reilly, J. P. *Anal. Chem.* **1990**, *62*, 1804.
(11) Gu, X.-B.; Wang, G.-J.; Huang, J.-H.; Han, K.-L.; He, G.-Z.; Lou, N.-Q. *J. Phys. Chem. A* **2001**, *105*, 354.
(12) Ichimura, T.; Mori, Y.; Shinohara, H.; Nishi, N. *Chem. Phys. Lett.* **1985**, *122*, 55.
(13) Ichimura, T.; Mori, Y.; Shinohara, H.; Nishi, N. *Chem. Phys. Lett.* **1986**, *125*, 263.
(14) Ichimura, T.; Mori, Y.; Shinohara, H.; Nishi, N. *J. Chem. Phys.* **1997**, *107*, 835.
(15) Zhu, R.-S.; Zhang, H.; Wang, G.-J.; Gu, X.-B.; Han, K.-L.; He, G.-Z.; Lou, N.-Q. *Chem. Phys. Lett.* **1999**, *248*, 285.
(16) Kadi, M.; Davidsson, J. *Chem. Phys. Lett.* **2003**, *378*, 172.
(17) Kadi, M.; Ivarsson, E.; Davidsson, J. *Chem. Phys. Lett.* **2004**, *384*, 35.
(18) Yuan, L.; Wang, Y.; Wang, L.; Bai, J.; He, G. *Sci. China, Ser. B: Chem.* **2004**, *47*, 283.
(19) Rasmusson, M.; Lindh, R.; Lascoux, N.; Tarnovsky, A. N.; Kadi, M.; Kuhn, O.; Sundstrom, V.; Akesson, E. *Chem. Phys. Lett.* **2002**, *367*, 759.
(20) Liu, Y.-J.; Persson, P.; Lunell, S. *J. Phys. Chem. A* **2004**, *108*, 2339.
(21) Liu, Y.-J.; Persson, P.; Lunell, S. *J. Chem. Phys.* **2004**, *121*, 11000.
(22) Liu, Y.-J.; Persson, P.; Karlsson, H. O.; Lunell, S.; Kadi, M.; Karlsson, D.; Davidsson, J. *J. Chem. Phys.* **2004**, *120*, 6502.
(23) Philis, J.; Bolovinos, A.; Andritsopoulos, G.; Pantos, E.; Tsekeris, P. *J. Phys. B: At. Mol. Phys.* **1981**, *14*, 3621.
(24) Loper, G. L.; Lee, E. K. C. *Chem. Phys. Lett.* **1972**, *13*, 140.
(25) Gilmore, E. H.; Gibson, G. E.; McClure, D. S. *J. Chem. Phys.* **1952**, *20*, 829.
(26) Varsanyi, G.; Holly, S.; Farago, T. *Spectrochim. Acta* **1963**, *19*, 683.
(27) Varsanyi, G.; Holly, S.; Farago, T. *Spectrochim. Acta* **1963**, *19*, 675.
(28) Varsanyi, G.; Holly, S.; Farago, T. *Spectrochim. Acta, Part A* **1963**, *19*, 669.

(29) Rao, R.; Aralakkanavar, M. K.; Katti, N. R.; Rao, K. S.; Shashidhar, M. A. *Indian J. Phys., B* **1990**, *64B*, 149.

(30) Sobolewski, A. L.; Domcke, W. *Chem. Phys.* **2000**, *259*, 181.

(31) Domcke, W., Yarkony, D. R., Koeppel, H., Eds. *Conical Intersections: Electronic Structure, Dynamics & Spectroscopy*; Advanced Series in Physical Chemistry; World Scientific Publishing Co.: Singapore, 2004, Vol. 15, p 2004.

(32) Davidsson, J.; Hansson, T.; Mukhtar, E. *J. Chem. Phys.* **1998**, *109*, 10740.

(33) Andersson, K.; P., F. M.; Lindh, R.; Malmqvist, P.-A.; Olsen, J.; Sadlej, A. J.; Widmark, P.-O. *MOLCAS version 5.4*, 5.4 ed.; University of Lund: Sweden, 2000.

(34) Roos, B. O.; Taylor, P. R.; Siegbahn, P. E. M. *Chem. Phys.* **1980**, *48*, 157.

(35) Roos, B. O.; Andersson, K.; Fuelscher, M. P.; Malmqvist, P.-A.; Andres, L. S.; Pierloot, K.; Merchan, M. *Adv. Chem. Phys.* **1996**, *93*, 219.

(36) Andersson, K.; Malmqvist, P.-A.; Roos, B. O.; Sadlej, A. J.; Wolinski, K. *J. Phys. Chem.* **1990**, *94*, 5483.

(37) Andersson, K.; Malmqvist, P.-A.; Roos, B. O. *J. Phys. Chem.* **1992**, *96*, 1218.

(38) Pierloot, K.; Dumez, B.; Widmark, P.-O.; Roos, B. O. *Theor. Chim. Acta* **1995**, *90*, 87.

(39) Barandiaran, Z.; Seijo, L. *Can. J. Chem.* **1992**, *70*, 409.

(40) Platt, J. R. *J. Chem. Phys.* **1949**, *17*, 484.

(41) Griffiths, J. A.; Jung, K.-W.; El-Sayed, M. A. *J. Phys. Chem.* **1996**, *100*, 7989.

(42) Kavita, K.; Das, P. K. *J. Chem. Phys.* **2002**, *117*, 2038.

(43) McGlynn, S. P.; Azumi, T.; Kinoshitra, M. *Molecular Spectroscopy of the Triplet State*; Prentice Hall: Englewood Cliffs, NJ, 1969.

(44) Zgierski, M. Z.; Fujiwara, T.; Lim, E. C. *J. Chem. Phys.* **2005**, *122*, 144312/1.